Extremophiles (2008) 12:461–469
DOI 10.1007/s00792-008-0152-z

ORIGINAL PAPER

Characterization of a thermostable dihydrodipicolinate synthase from *Thermoanaerobacter tengcongensis*

Suzanne Wolterink-van Loo · Mark Levisson · Maud C. Cabrières · Maurice C. R. Franssen · John van der Oost

Received: 5 October 2007 / Accepted: 12 February 2008 / Published online: 15 March 2008

Abstract Dihydrodipicolinate synthase (DHDPS) catalyses the first reaction of the (*S*)-lysine biosynthesis pathway in bacteria and plants. The hypothetical gene for dihydrodipicolinate synthase (*dapA*) of *Thermoanaerobacter tengcongensis* was found in a cluster containing several genes of the diaminopimelate lysine–synthesis pathway. The *dapA* gene was cloned in *Escherichia coli*, DHDPS was subsequently produced and purified to homogeneity. The *T. tengcongensis* DHDPS was found to be thermostable ($T_{0.5} = 3$ h at 90°C). The specific condensation of pyruvate and (*S*)-aspartate-β -semialdehyde was catalyzed optimally at 80°C at pH 8.0. Enzyme kinetics were determined at 60°C, as close as possible to in vivo conditions. The established kinetic parameters were in the same range as for example *E. coli* dihydrodipicolinate synthase. The specific activity of the *T. tengcongensis* DHDPS was relatively high even at 30°C. Like most dihydrodipicolinate synthases known at present, the DHDPS of *T. tengcongensis* seems to be a tetramer. A structural model reveals that the active site is well conserved. The binding site of the allosteric inhibitor lysine appears not to be conserved, which agrees with the fact that the DHDPS of *T. tengcongensis* is not inhibited by lysine under physiological conditions.

Keywords Enzymes · Dihydrodipicolinate synthase · Thermophile · Lysine biosynthesis · *Thermoanaerobacter tengcongensis*

Abbreviations

DAP	Diaminopimelate
DIBAL	Di*iso*butylaluminium hydride
DHDP	Dihydrodipicolinate
DHDPR	Dihydrodipicolinate reductase
DHDPS	Dihydrodipicolinate synthase
HTPA	(4*S*)-4–hydroxy-2,3,4,5-tetrahydro-(2*S*)-dipicolinic acid
NAL	*N*-acetylneuraminate lyase
(*S*)-ASA	(*S*)-aspartate-β-semialdehyde
TCA	Trichloroacetic acid

Introduction

Dihydrodipicolinate synthase (DHDPS) (EC 4.2.1.52) is the key enzyme in lysine biosynthesis via the diaminopimelate pathway, which is used by bacteria (Shedlarski and Gilvarg 1970; Cremer et al. 1988; Blagova et al. 2006; Tsujimoto et al. 2006), some phycomycetes and higher plants (Frisch et al. 1991; Dereppe et al. 1992; Vauterin and Jacobs 1994; Ghislain et al. 1995). The enzyme catalyses the condensation of (*S*)-aspartate-β-semialdehyde ((*S*)-ASA) and pyruvate to 2,3-dihydrodipicolinic acid (Yugari and Gilvarg 1965) (Fig. 1). Blickling et al. (1997b) reported (4*S*)-4-hydroxy-2,3,4,5-tetrahydro-(2*S*)-dipicolinic acid (HTPA) as direct product

Communicated by G. Antranikian.

S. Wolterink-van Loo · M. Levisson · J. van der Oost (✉)
Laboratory of Microbiology, Wageningen University,
Dreijenplein 10, 6703 HB Wageningen, The Netherlands
e-mail: john.vanderoost@wur.nl

M. C. Cabrières · M. C. R. Franssen
Laboratory of Organic Chemistry, Wageningen University,
Dreijenplein 8, 6703 HB Wageningen, The Netherlands

of this reaction. In all cases examined, the reaction proceeds via a ping-pong mechanism in which pyruvate binds as a Schiff-base to the amino group of a lysine residue in the active site of the enzyme. Then, (*S*)-ASA binds to enzyme-bound enamine of pyruvate, and after transamination and cyclization the product is released (Blickling et al. 1997b). Subsequently 2,3-dihydrodipicolinate (DHDP) may be formed spontaneously under physiological conditions (Blickling et al. 1997b). It is generally assumed that DHDP is substrate for dihydrodipicolinate reductase (Scapin et al. 1997; Wang et al. 1997) (Fig. 1).

According to the classification of Grazi et al. (1962), DHDPS is a type-I aldolase belonging to the Neuraminate lyase (NAL) superfamily (Choi et al. 2006). The amino acid sequences of DHDPSs from different organisms are well conserved. Most DHDPS-structures known to date have a homotetrameric quaternary structure (Mirwaldt et al. 1995; Blickling et al. 1997a; Blagova et al. 2006; Pearce et al. 2006), with each monomer consisting of an $(\alpha/\beta)_8$ barrel and a C-terminal alpha-helical domain.

DHDPS in higher plants is generally feedback inhibited by low concentrations of (*S*)-lysine (µmolar range, $K_i = 11–51$ µM) (Mazelis et al. 1977; Kumpaisal et al. 1987; Frisch et al. 1991; Dereppe et al. 1992; Ghislain et al. 1995), while their counterparts in gram-negative bacteria are only moderately inhibited ($K_i = 0.4$ mM) (Laber et al. 1992; Karsten 1997). Interestingly, DHDP synthases from gram-positive bacteria have shown to be insensitive to (*S*)-lysine (Stahly 1969; Hoganson and Stahly 1975; Cahyanto et al. 2006). Recently, residues that are probably responsible for binding of the (*S*)-lysine effector in *E. coli* DHDPS have been identified (Dobson et al. 2005).

In this study we analyzed a gene cluster encoding enzymes that participate in the diaminopimelate pathway for lysine synthesis, present in *Thermoanaerobacter tengcongensis*, a gram-positive, thermophilic bacterium with optimal growth at 75°C (Xue et al. 2001). The first two genes of this pathway (*dapA* & *dapB*) of *T. tengcongensis* are cloned and expressed in *E. coli*. The *dapA* gene is coding for the DHDPS, which is characterized in detail and compared to other known DHDP synthases.

Materials and methods

(*S*)-ASA synthesis

(S)-2-tert-Butoxycarbonylamino-N-methoxy-N-methyl-succinamic acid tert-butyl ester (1) (Wernic et al. 1989)

All glassware was dried 24 h in an oven at 140°C before use and the dichloromethane was freshly distilled. To a stirred solution of *N*-Boc-Asp-OtBu (1eq., 17 mmol, 5 g) in dry dichloromethane (175 mL) under nitrogen atmosphere and at room temperature was added triethylamine (1.1 eq., 19 mmol, 3 mL) and solid (benzotriazol-1-yloxy)tris(dimethylamino)phosphonium hexafluorophosphate (BOP.PF_6, 1.1 eq., 19 mmol, 8.40 g), giving a homogeneous mixture. After 5 min, solid *N*,*O*-dimethylhydroxylamine hydrochloride (1.1 eq., 19 mmol, 2 g) was added, followed by another portion of triethylamine (1.1 eq., 3 mL). After 10 min, the suspension was completely dissolved. The mixture was stirred at room temperature for 5 h. The reaction was followed by TLC on silica with petroleum ether:EtOAc 1:1 as eluent. The solution was then washed with HCl (1 M, 3 × 50 mL), H_2O (1 × 50 mL), $NaHCO_3$ (1 M, 2 × 50 mL). The organic layers were dried with Na_2SO_4 and the solvent was evaporated in vacuo ($T < 30$°C, 350 mmHg). A crude yellowish oil was obtained which was purified on a silica chromatography column using petroleum ether:EtOAc 6:4 as eluent. A colorless oil was obtained (5.50 g, 96%).

^{1}H NMR (200 MHz) in DMSO: δ 1.36 (s, 18H), 2.73 (d, 2H), 3.07 (s, 3H), 3.65 (s, 3H), 4.20 (m, 1H), 7.10 (d, 1H).

(S)-2-tert-Butoxycarbonylamino-4-oxo-butyric acid tert-butyl ester (2) (Wernic et al. 1989)

All glassware was dried 24 h in an oven at 140°C before use and THF was freshly distilled. To a stirred solution of **1** (Fig. 2) (1 eq., 7.52 mmol, 2.5 g) in dry THF (100 mL) at -78°C and under nitrogen atmosphere was added dropwise a solution of di*iso*butylaluminium hydride (DIBAL) in dichloromethane (1 M, 1.5 eq., 12.0 mmol, 12 mL) in about 30 min. The reaction was stirred in these conditions for 3 h and the progress was followed by TLC on silica

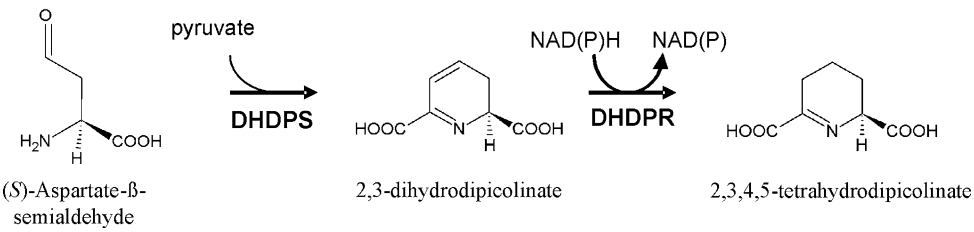

Fig. 1 Reactions catalyzed by DHDPS (EC 4.2.1.52) and DHDPR (EC 1.3.1.26). According to (Blickling et al. 1997b) the immediate product formed by DHDPS is (4*S*)-4-hydroxy-2,3,4,5-tetrahydro-(2*S*)-dipicolinic acid

with petroleum ether:ether 1:1 as eluent. The reaction mixture was then partitioned between ether (150 mL) and a solution of $NaHSO_4$ (0.35 M in water, 100 mL). The aqueous layer was extracted with ether (3 × 50 mL). The combined organic layers were washed successively with solutions of HCl (1 M, 3 × 50 mL), $NaHCO_3$ (1 M, 3 × 50 mL) and brine (3 × 100 mL) and dried using Na_2SO_4. The solvent was removed *in vacuo* (RT, $650 < P < 50$ mmHg). A colorless oil was obtained which crystallized by standing overnight at room temperature. In case a mixture of product and starting material was obtained, a purification on silica chromatography column with petroleum ether/EtOAc as eluent was performed. The solid was purified by recrystallization in cold *n*-hexane (0.90 g, 44 %).

^{1}H NMR (300 MHz) in $CDCl_3$: δ 1.42 (s, 18H), 2.95 (t, 2H), 4.40 (m, 1H), 5.29 (d, 1H), 9.6 ppm (s, 1H).

^{13}C NMR (300 MHz) in $CDCl_3$: δ 28.2 (CH_3), 28.7 (CH_3), 46.8 (CH_2), 49.7 (CH), 155.7 (COOtBu), 170.3 (NHCO), 199.7 (CHO).

(S)-2-Amino-4,4-dihydroxy-butyric acid, trifluoroacetate salt [(S)-ASA hydrate, TFA salt] (Roberts et al. 2003)

All glassware was dried 24 h in an oven at 140°C before use and dichloromethane was distilled and dried on molecular sieves 3 Å before use. A solution of **2** (Fig. 2) (0.6 g, 2.2 mmol) was stirred in dry dichloromethane (15 mL) under nitrogen atmosphere for 15 min. Then, trifluoroacetic acid (15 mL) was added rapidly. The reaction mixture was stirred 2.5 h after addition. The solvent was evaporated in vacuo (rt, 200 mmHg). The yellow oily residue obtained was partitioned between ethyl acetate (60 mL) and deionized water (60 mL). An emulsion was observed which separated upon standing. After decantation, the aqueous phase was washed twice with ethyl acetate (2 × 60 mL) and the water was evaporated in vacuo (rt, $P < 60$ mmHg) but not to dryness to avoid the removal of TFA and therefore the polymerization of the product. The presence of polymer can be checked by TLC.

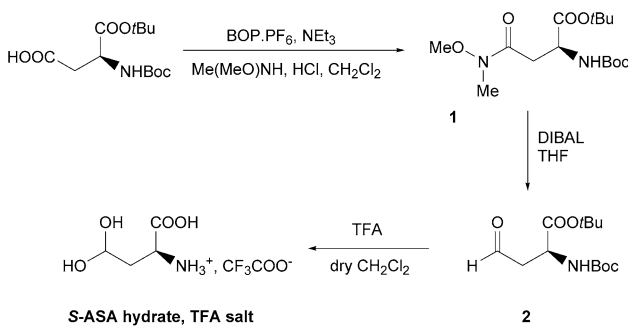

Fig. 2 Synthetic scheme of (*S*)-ASA

A yellow solution was obtained ($y = 98\%$). The concentration of the product in water was determined by ^{1}H and ^{13}C NMR with fumaric acid as internal standard. $[\alpha]^{20}_D = +3.73$ ($c = 1.5$, H_2O), lit [2] +3.33 ($c = 1.5$, H_2O).

^{1}H NMR (200 MHz) in D_2O: δ 2.0 (m, 2H), 3.9 (dd, 1H), 5.1 (t, 1H), 1.2 (s, presence of residual *t*-butanol).

^{13}C NMR (200 MHz) in D_2O: δ 38.7 (CH_2-C3), 52.3 (CH-C2), 90.3 (CH-C4), 119.0 (*q*, CF_3), 165.0 (CF_3C), 174.0 (COOH), 29.0 ppm (*tert*-BuOH).

Concentration determination by ^{1}H NMR

The (*S*)-ASA solution (30 mg) and fumaric acid solution (200 µL, 5 g L^{-1}, 25 mg dissolved in 5 mL of D_2O) were put in a volumetric flask of 2 mL. This solution was used to fill the NMR tube. The NMR spectrum was determined with suppression of the water signal. After comparison of the signal intensity of both compounds, a concentration of 81% w/v was found.

Cloning

The predicted *T. tengcongensis* (DSM 15242^T, JCM11007) genes *dapA* (TTE0832; Genbank Identifier 20515826) and *dapB* (TTE0831: Genbank Identifier 20515825) were PCR-amplified from genomic DNA of *T. tengcongensis* using Pfu DNA-polymerase (Stratagene) and primer pairs BG1758-1759 (BG1758-sense: 5′-GCGCCCATGGCACC TGTATTTAAAGGTTCATGTGTGGC-3′; BG1759-antisense: 5′-GCGCCTCGAGATTTTCCTCCTTTAAAAG GCCCATACTGC-3′) and BG1953-1954 (BG1953-sense: 5′-CGCGCTCATGATGATAAGGCTAATAATCCAC-3′; BG1954 - antisense: 5′-CGCGCGTCGACTCATCCTTTC TTTACAAGGTCTTC-3′) respectively. The *dapA* gene was cloned into a pET24d vector, as a NcoI/XhoI restriction fragment, resulting in vector pWUR194, which, after expression, results in a protein with an extra alanine at the second place and a C-terminal His-tag: LEHHHHHH. The *dapB* gene was cloned into the pET24d vector using BspHI (in NcoI) and SalI resulting in vector pWUR213, encoding the 'wild type' protein (without a His-tag). Both plasmids were transformed to *E. coli* BL21(DE3).

Production and purification of enzymes

Production of *T. tengcongensis* DHDPS (Tte-DHDPS) was performed using 1 L LB culture, supplemented with 50 µg/mL kanamycin, inoculated with *E. coli* BL21(DE3) containing the pWUR194. After 4 h of growth (37°C with shaking), the culture was induced with 1 mM IPTG (isopropyl-β-D-thiogalactopyranoside) and growth was continued overnight at 37°C. The cells were harvested by centrifugation (3,800×*g*, 10 min), resuspended in 20 mL

50 mM sodium phosphate buffer pH 7.0–0.5 M NaCl and lysed using a French press. After centrifugation (27,000×*g*, 20 min) the soluble protein fraction was incubated at 70°C for 30 min. This was centrifuged (48,000×*g*, 30 min) to obtain the heat stable cell free extract (HSCFE). The Tte-DHDPS was further purified on an ÄKTA FLPC (Amersham Pharmacia Biotech), using affinity chromatography (Nickel-chelating Superose column), and a one-step elution with 50 mM sodium phosphate buffer pH 7.5, containing 0.5 M NaCl and 0.5 M imidazole. Fractions containing Tte-DHDPS were pooled and then applied to a desalting column (HiPrep 26/10, Pharmacia Biotech), using 50 mM sodium phosphate pH 7.0, 50 mM NaCl, to remove the imidazole.

Thermoanaerobacter tengcongensis DHDPR (Tte-DHDPR) was produced in a similar way, using 0.15 mM IPTG for induction. Cells were resuspended in 30 mL 90 mM HEPES, 160 mM KCl, pH 7.0–the heat incubation was shortened to 15 min. Tte-DHDPR was purified on an ÄKTA FLPC using anion-exchange chromatography (Q-sepharose; 20 mM Tris-HCl, pH 8.5, gradient 0–1 M NaCl, DHDPR in flowthrough). Fractions containing Tte-DHDPR were subsequently desalted, and further purification was performed using anion-exchange chromatography (Mon-oQ; 20 mM Tris/HCl pH 8.5, gradient 0–1 M NaCl, elution at 0.28 M). Proteins were analyzed on a 12% SDS-PAGE after staining with Coomassie blue.

Enzyme assays

Pyruvate depletion assay

DHDPS activity was measured by assaying the remaining pyruvate in a standardized lactate dehydrogenase (LDH) assay in duplo. Reactions of 1 mL volume containing 50 mM sodium phosphate buffer, pH 6, 0.5 mM pyruvate, 0.5 mM (*S*)-ASA and an appropriate amount of enzyme were incubated at 60°C for 5–10 min. The reaction was stopped by adding 100 µL 12% trichloroacetic acid (TCA) and precipitated protein was removed by centrifugation (16,000×*g*, 10 min). From a mixture containing 100 mM Tris/HCl pH 7.5, 0.16 mM NADH and 300 µL sample the starting absorbance at 340 nm was read. After adding 3 units of LDH and incubating for 5 min, the absorbance was read again. The absorbance difference in NADH (molecular extinction coefficient 6.22 mM^{-1} cm^{-1}; (Horecker and Kornberg 1948)) was used to calculate the amount of pyruvate left in the reaction mixture.

Substrate specificity was tested as follows. Different aldehydes (20 mM) were incubated with pyruvate (10 mM) and 25 µg DHDPS in a 100 µl volume (buffered in 50 mM sodium phosphate/50 mM sodium citrate pH 8.0) for 1 h at 60°C. Reactions were stopped by adding 10 µL 12% TCA. A 16 µL sample was used to determine the remaining pyruvate as described above. Reactions with the aldoses as substrates were additionally analyzed with a thiobarbituric acid–assay as described previously (Wolterink-van Loo et al. 2007).

Coupled assay to DHDPR

DHDPS activity was measured in a continuous assay, using DHDPR, as previously described by Yugari and Gilvarg (1965). Standard incubations contained 50 mM sodium phosphate/50 mM citrate buffer pH 8.0, 10 mM sodium pyruvate, 0.16 mM β-NADH, an excess of Tte-DHDPR (usually 30 µg) and an appropriate amount of Tte-DHDPS (0.1–1 µg) in 1 mL volume in a quartz cuvet. This mixture was heated up to 60°C for 5 min, the reaction was then initiated by adding 1 mM (*S*)-ASA. The reaction was followed by measuring the absorption decrease of β-NADH at 334 nm (molecular extinction coefficient: 6.18×10^3 M^{-1} cm^{-1} (Ziegenhorn et al. 1976)). Measurements were performed in duplicate or triplicate. (*S*)-ASA was stable for the time taken in the experiments up to 60°C (initial velocity taken within 30 s). Kinetic data are expressed in U/mg, where 1 unit is equal to 1 µmol of NADH oxidized per sec. When kinetic parameters for (*S*)-ASA were determined, the concentration varied between 0.1 and 8.0 mM and pyruvate was present in excess at 20 mM, while the kinetic parameters for pyruvate were determined by varying the concentration between 0.2 and 20 mM, using 2 mM (*S*)-ASA. Michaelis Menten kinetics were modeled using TableCurve 2D and the following equations:

$$v = V_{max} \times [S]/(K_M + [S])$$

$$v = V_{max} \times [S]/(K_M + [S] + ([S]^2/K_i))$$

Where v is the enzyme activity at a particular substrate concentration ([*S*]) and K_i the inhibition constant of (*S*)-ASA.

Optimum pH and temperature

The assays were performed as the standard coupled assay, with replacement of the buffer with similar ionic strength to vary the pH (pH 4.0–8.0: phosphate-citrate buffer, pH 8.0–9.5: glycine). To determine the optimal temperature, the assay temperature was varied from 30 to 90°C.

Lysine inhibition

Inhibition caused by (*S*)-lysine was tested by performing the standard coupled assay and adding increasing amounts of (*S*)-lysine (0–200 mM).

Heat stability

Aliquots of 12.6 μg/mL DHDPS in assay buffer were incubated at 90°C, removed at time intervals (up to 5 h) and cooled rapidly to 0°C. Residual activity was measured using the standard coupled assay described above.

Alignments

Protein sequence alignments were made using MegAline from DNASTAR and manually checked using GeneDoc. A structural model was made by submitting the Tte-DHDPS protein sequence to PHYRE (Protein Homology/analogY Recognition Engine). The models based on *E. coli* and *T. maritima* DHDPS had low E-values of 4.3e-44 and 1.8e-43. The model (monomer of *T. tengcongensis* DHDPS) based on *E. coli* DHDPS was used further. PyMol was used to fit the model on the structures of *E. coli* and *T. maritima* DHDPS for comparison of active sites and possible binding site of lysine.

Results and discussion

Genomic location of the lysine synthesis genes

The diaminopimelate (DAP) pathway towards (*S*)-lysine includes nine consecutive steps, starting with (*S*)-aspartate as a precursor. The first two steps, involving an aspartate kinase and an aspartate-semialdehyde dehydrogenase, are shared with the threonine biosynthesis pathway. In *Thermotoga maritima* and *T. tengcongensis* part of these (non-characterized/hypothetical) *dap*-genes are clustered in an operon-like structure (Fig. 3). In *T. tengcongensis* the clustered genes include the aspartate-semialdehyde dehydrogenase gene (TTE0833, *asd*), the dihydrodipicolinate synthase gene (TTE0832, *dapA*), the dihydrodipicolinate reductase (TTE0831, *dapB*) and the *N*-succinyl transferase gene (TTE0830, *dapD*). In the corresponding cluster of *T. maritima* (TM1517-1523) three additional genes are present: *lysC*, encoding the enzyme that catalyses the first step of the pathway and *dapF* and *lysA* (responsible for the last two steps). Additionally, related gene clusters are present in C*lostridia* species comprising *asd*, *dapA* and *dapB* (Fig. 3). The remaining *T. tengcongensis* enzymes in the DAP-pathway, for which (hypothetical) genes are missing in this cluster, had alternative (hypothetical) genes elsewhere on the genomes, based on either KEGG PATHWAY analysis or BLAST analysis: *lysC*; TTE1382, *dapC*; TTE2440, *dapE*; TTE1746, *dapF*; TTE1514, *lysA*; TTE0210.

Biochemical characterization

The *dapA* and *dapB* genes of the *T. tengcongensis* genome, coding for DHDP synthase and DHDP reductase, were cloned and expressed in *E. coli* and purified to homogeneity (Fig. 4a), using a heat incubation step and additional chromatography (as described in "Materials and methods"). The DHDP synthase activity was first analyzed with a pyruvate depletion assay to test dihydrodipicolinate synthase activity during purification.

Biochemical characterization of *T. tengcongensis* (Tte-DHDPS) (Table 1) was performed using a coupled assay, using an excess of *T. tengcongensis* DHDP-reductase (Tte-DHDPR) and following the oxidation of β-NADH. Optimal activity was found at pH 8.0, which is similar to that of the *E. coli* enzyme (Eco-DHDPS) (Shedlarski and Gilvarg 1970) and some plant DHDP synthases (Kumpaisal et al. 1987; Dereppe et al. 1992; Tam et al. 2004). Furthermore, an attempt was made to measure the temperature optimum. It was necessary to keep the assay time very short due to instability of (*S*)-ASA (Coulter et al. 1996). Using this method the highest specific activity could be measured at 80°C (Fig. 4b). At physiological temperature (75°C), under the conditions used, (*S*)-ASA did completely disappear within 7 min as tested with residual DHDPS-activity. Obviously the stability of (*S*)-ASA is sufficient for metabolic conversion in vivo due to high turnover, and possibly because of the presence of compatible solutes. Furthermore, although no experimental evidence is yet available, the enzymes involved in (*S*)-lysine synthesis could be organized in functional complexes for efficient transfer of intermediates, a phenomenon called metabolic channeling (Massant et al. 2002).

Unlike a recent analysis of *T. maritima* DHDPS by (Pearce et al. 2006), we decided to perform activity measurements at elevated temperature (60°C) to characterize *T. tengcongensis* DHDPS, closer to its in vivo conditions. During characterization, the reaction time was kept very short and the reaction was initiated by adding (*S*)-ASA. As such, it was possible to determine initial reaction velocities. When varying the pyruvate concentration, the apparent V_{max} was 17.8 (±0.3) U/mg, with the K_M^{app} for pyruvate being 0.85 (±0.05) mM, using 2 mM (*S*)-ASA. When the (*S*)-ASA concentration was varied, using 20 mM pyruvate, the apparent V_{max} was 19.0 (±0.8) U/mg and the K_M^{app} for (*S*)-ASA 0.38 (±0.05) mM. When modeled with substrate inhibition: $K^{app}_{M(S)-ASA}$ was 0.92 (±0.13) mM, with inhibition constant, $K_{i(S)\text{-}ASA} = 4.7$ (±0.8) mM. These kinetic values at 60°C are somewhat higher compared to those of Eco-DHDPS and Tma-DHDPS, which were determined at 30°C (Table 1). Most likely, this depends on the different assay temperature used here, as in previous enzyme

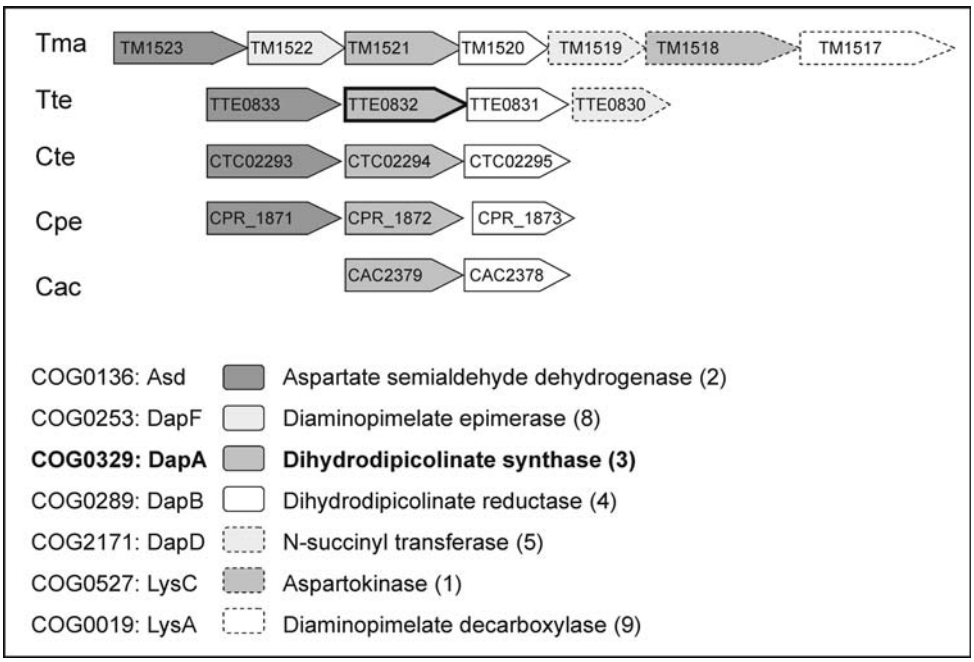

Fig. 3 Gene clusters of the diaminopimelate pathway in bacteria. Comparison of clustered genes of lysine synthesis in *T. tengcongensis* (Tte) and *T. maritima* (Tma), *Clostridium tetani* (Cte), *C. perfringens* (Cpe), *C. acetobutylicum* (Cac). *Genes* are indicated by their systematic gene name

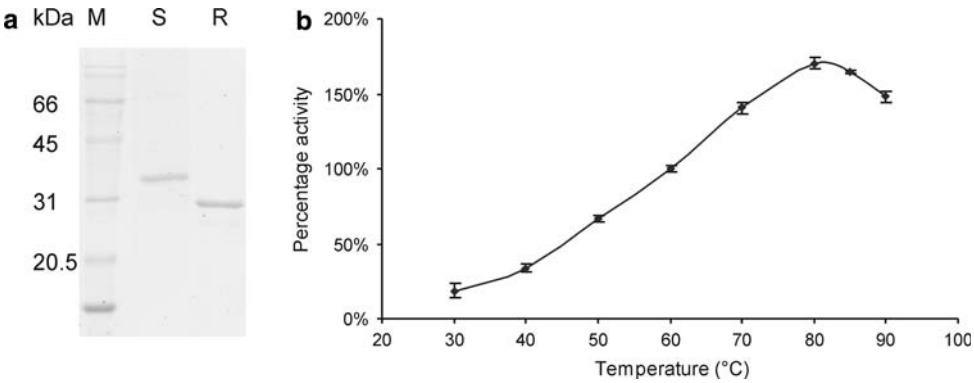

Fig. 4 Expression and activity of DHDPS. **a** SDS-PAGE of purified DHDPS and DHDPR. M; marker proteins, S; DHDPS, R: DHDPR. **b** Temperature curve of relative activity of Tte-DHDPS. Absolute activity at 60°C was 15.7 U/mg, which is set at 100%

analyses it has been shown, that the K_M of an enzyme can either increase or decrease with increasing temperature (Vieille et al. 1995). The different K_M values here are nevertheless still in range with the K_M values reported for other DHDPSs (Dereppe et al. 1992; Dobson et al. 2004a; Tam et al. 2004). Remarkably, specific activity of Tte-DHDPS at 30°C (3.3 U/mg) is higher than the V_{max} of *E. coli* DHDPS (0.58 U/mg) (Dobson et al. 2004a) and of the recently characterized *T. maritima* 1.01 U/mg at 30°C (Pearce et al. 2006).

Different studies of DHDP synthases reported substrate inhibition by (*S*)-ASA (Stahly 1969; Kumpaisal et al. 1987; Karsten 1997), while others, knowing about this possible problem just avoided high concentrations of this substrate (Tam et al. 2004). Dobson et al. (2004a) state that this inhibition problem is caused by a side product formation during (*S*)-ASA synthesis by ozonolysis; other methods (Tudor et al. 1993; Coulter et al. 1996; Roberts et al. 2003) showed no inhibition. Our method of (*S*)-ASA synthesis is similar to that of Roberts et al. (2003) and therefore should not give any inhibition problems. However at concentrations of (*S*)-ASA higher than 2 mM, enzyme activity decreased. The latter coincided with formation of an orange color, which indicates some side reactions during incubation, probably due to the (relatively) high temperature used in our studies. It is unclear if the lower activity is caused by this orange compound or by substrate inhibition.

Substrate specificity

In order to investigate the substrate specificity of Tte-DHDPS a range of commercially available aldehydes were tested for their ability to replace (*S*)-ASA in the

Table 1 Biochemical data for bacterial dihydrodipicolinate synthases

	Tte-DHDPS	Eco-DHDPS	Tma-DHDPS
pH optimum	8.0	8.0	ND
Temperature optimum	85°C	30°C	ND
$V^{app}_{max(pyr)}$	17.8 (0.3) U/mg	0.58 U/mg[b]	1.01 U/mg[a]
$K^{app}_{m(pyr)}$	0.85 (0.05) mM	0.25 mM[b]	0.053 mM[a]
$V^{app}_{max(ASA)}$	19.0 (0.8) U/mg	0.58 U/mg[b]	1.01 U/mg[a]
$K^{app}_{m(ASA)}$	0.38 (0.05) mM	0.11 mM[b]	0.16 mM[a]
K_i (lysine)	180 mM	3.9/0.32 mM	>>4 mM[a]
$T_{1/2}$ (90°C)	175 min	<30 s[a]	>400 min[a]

One unit (U) of enzyme activity is equal to the loss of 1 μmol_{NADH} s^{-1}

[a] Data from Pearce et al. (2006) true K_m values determined

[b] Data from Dobson et al. (2004a), true K_m values determined

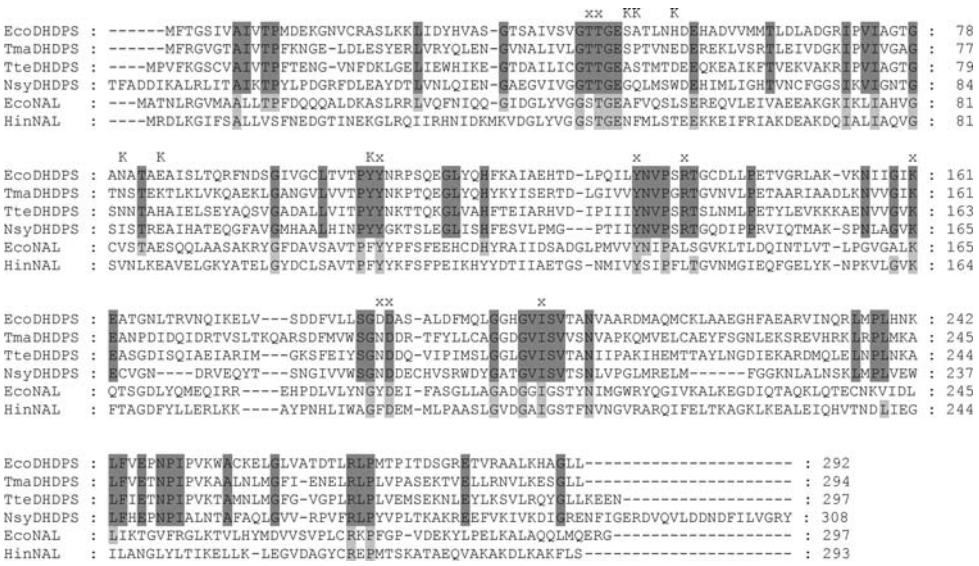

Fig. 5 Alignment of Tte-DHDPS. Alignment of different dihydrodipicolinate synthases and Neuraminate lyases. Eco; *E. coli*, Tma; *T. maritima*, Tte; *T. tengcongensis*, Nsy; *Nicotiana sylvestris*, Hin; *Heamophilus influenzae*. Catalytic residues are shown with *x*. Residues involved in (*S*)-lysine binding in *E. coli* are indicated with *K*. Conserved residues are highlighted in *grey* in DHDPS sequences, and in a *lighter grey* in Neuraminate lyases

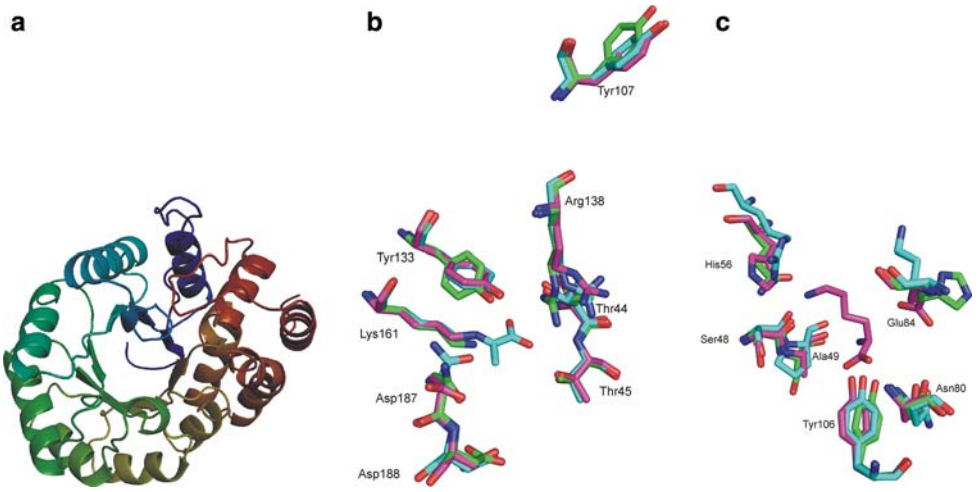

Fig. 6 Structural analysis of Tte-DHDPS. **a** Tte-DHDPS monomer, top view. **b** Active site residues: Overlay of the active sites of Tte-DHDPS (model) (*green*), Tma-DHDPS (including bound pyruvate) (*cyan*) and Eco-DHDPS (*magenta*), numbering of residues as in Eco-DHDPS. **c** Site of binding of (*S*)-lysine in *E. coli*. Overlay of the (*S*)-lysine binding site of Eco-DHDPS (*magenta*), Tma-DHDPS (*cyan*) and Tte-DHDPS (model) (*green*), numbering of residues as in Eco-DHDPS

condensation reaction. None of the tested 3-carbon aldehydes (propionaldehyde and D,L-glyceraldehyde), 4-carbon aldehydes (D-erythrose, L-erythrose, D-threose, L-threose) or 5-carbon aldehydes (D-arabinose, L-arabinose, D-ribose, D-xylose) could replace (*S*)-ASA. Of the 2-carbon aldehydes (acetaldehyde, glycolaldehyde, glyoxylate), Tte-DHDPS only showed significant activity with glycolaldehyde at a very low rate ~0.005% relative to the reaction with (*S*)-ASA. Hence, the Tte-DHDPS enzyme is very specific for (*S*)-ASA, in agreement with reports on Eco-DHDPS and DHDPS of wheat, which were inactive on (*R*)-ASA (Kumpaisal et al. 1987; Dobson et al. 2004a).

Structurally conserved features

Alignment of Tte-DHDPS with *E. coli*, *T. maritima* and *Nicotiana sylvestris* DHDPSs and Neuraminate lyases (NALs) from *E. coli* and *Haemophilus influenzae* showed that Tte-DHDPS has high homology with known DHDPSs, especially with Tma-DHDPS (57% identity) and Eco-DHDPS (54% identity) (Fig. 5). The active site lysine residue is present in all aligned DHDPSs and NALs as is the catalytic triad, consisting of Thr44, Tyr107 and Tyr133 (*E. coli* numbering), previously shown by Dobson et al. (2004b). The NALs only miss the Thr44, which is conservatively replaced by a serine (Fig. 5). A structural model of Tte-DHDPS (Fig. 6a) (model of the monomer) showed that the active site residues were structurally conserved as well (Fig. 6b) within DHDPSs from *T. tengcongensis*, *T. maritima* and *E. coli*. The calculated size of the Tte-DHDPS monomer (including the His-tag) is 34 kDa; analysis with size exclusion chromatography revealed a dominant form of ca. 150 kDa, indicating a tetramer in solution, which is similar to oligomeric states of most DHDP synthases known to date (Blickling et al. 1997a; Dobson et al. 2004b; Pearce et al. 2006).

Lysine inhibition

DHDPS of gram-positive bacteria is generally not inhibited by lysine (Stahly 1969; Hoganson and Stahly 1975; Cahyanto et al. 2006), and Tte-DHDPS is not an exception in that respect. When testing for possible lysine inhibition, adding lysine up to a concentration of 20 mM did not lead to detectable difference in activity. Only when extremely high concentrations of lysine were used, an apparent inhibition constant could be determined ($K_{i(\text{lysine})} = 180$ mM). In Eco-DHDPS, which is inhibited by lysine, the mode of binding was determined by co-crystallization (Dobson et al. 2005). When looking at the residues involved in binding in Eco-DHDPS, only the Tyr106 is conserved in all DHDPSs and Asn80 is conserved in nearly all bacterial DHDPSs (including Tte-DHDPS). Ser48 seems to be present in gram-negative DHDPSs, Ala49, His56 and Glu84 are less conserved (Fig. 5), but are present in some gram-negative DHDPSs. This might indicate that inhibition of DHDPS by lysine in gram-negatives is similar to the mechanism in Eco-DHDPS. From a structural overlay of the lysine binding site of Eco-DHDPS and aligned residues in Tte-DHDPS and Tma-DHDPS it is clear that only few residues are conserved (Fig. 6c). According to Dobson et al. (2005), the nitrogen of His56 and the carbonyl oxygen of Glu84 are within bonding distance in Eco-DHDPS, which are replaced by other residues in Tte-DHDPS and Tma-DHDPS. Those residues apparently do not bind the lysine, leading to the insensitivity of these two DHDP synthases for (*S*)-lysine.

Acknowledgments We want to thank Dr. Gabriella M. Preda (West University of Timisoara) for the synthesis of a batch of (*S*)-ASA. This research is performed as part of the IBOS Programme (Integration of Biosynthesis & Organic Synthesis) of Advanced Chemical Technologies for Sustainability (ACTS).

References

Blagova E, Levdikov V, Milioti N, Fogg MJ, Kalliomaa AK, Brannigan JA, Wilson KS, Wilkinson AJ (2006) Crystal structure of dihydrodipicolinate synthase (BA3935) from Bacillus anthracis at 1.94 A resolution. Proteins 62:297–301

Blickling S, Beisel HG, Bozic D, Knablein J, Laber B, Huber R (1997a) Structure of dihydrodipicolinate synthase of *Nicotiana sylvestris* reveals novel quaternary structure. J Mol Biol 274:608–621

Blickling S, Renner C, Laber B, Pohlenz HD, Holak TA, Huber R (1997b) Reaction mechanism of *Escherichia coli* dihydrodipicolinate synthase investigated by X-ray crystallography and NMR spectroscopy. Biochemistry 36:24–33

Cahyanto MN, Kawasaki H, Nagashio M, Fujiyama K, Seki T (2006) Regulation of aspartokinase, aspartate semialdehyde dehydrogenase, dihydrodipicolinate synthase and dihydrodipicolinate reductase in *Lactobacillus plantarum*. Microbiology 152:105–112

Choi KH, Lai V, Foster CE, Morris AJ, Tolan DR, Allen KN (2006) New superfamily members identified for Schiff-base enzymes based on verification of catalytically essential residues. Biochemistry 45:8546–8555

Coulter CV, Gerrard JA, Kraunsoe JAE, Moore DJ, Pratt AJ (1996) (*S*)-Aspartate semi-aldehyde: synthetic and structural studies. Tetrahedron 52:7127–7136

Cremer J, Treptow C, Eggeling L, Sahm H (1988) Regulation of enzymes of lysine biosynthesis in *Corynebacterium glutamicum*. J Gen Microbiol 134:3221–3229

Dereppe C, Bold G, Ghisalba O, Ebert E, Schar HP (1992) Purification and characterization of dihydrodipicolinate synthase from pea. Plant Physiol 98:813–821

Dobson RC, Gerrard JA, Pearce FG (2004a) Dihydrodipicolinate synthase is not inhibited by its substrate, (*S*)-aspartate beta-semialdehyde. Biochem J 377:757–762

Dobson RC, Valegard K, Gerrard JA (2004b) The crystal structure of three site-directed mutants of *Escherichia coli* dihydrodipicolinate synthase: further evidence for a catalytic triad. J Mol Biol 338:329–339

Dobson RC, Griffin MD, Jameson GB, Gerrard JA (2005) The crystal structures of native and (*S*)-lysine-bound dihydrodipicolinate synthase from *Escherichia coli* with improved resolution show new features of biological significance. Acta crystallogr Sect D 61:1116–1124

Frisch DA, Gengenbach BG, Tommey AM, Sellner JM, Somers DA, Myers DE (1991) Isolation and characterization of dihydrodipicolinate synthase from maize. Plant Physiol 96:444–452

Ghislain M, Frankard V, Jacobs M (1995) A dinucleotide mutation in dihydrodipicolinate synthase of *Nicotiana sylvestris* leads to lysine overproduction. Plant J 8:733–743

Grazi E, Rowley PT, Cheng T, Tchola O, Horecker BL (1962) The mechanism of action of aldolases. III. Schiff base formation with lysine. Biochem Biophys Res Commun 9:38–43

Hoganson DA, Stahly DP (1975) Regulation of dihydrodipicolinate synthase during growth and sporulation of *Bacillus cereus*. J Bacteriol 124:1344–1350

Horecker BL, Kornberg A (1948) The extinction coefficients of the reduced band of pyridin nucleotides. J Biol Chem 175:385–390

Karsten WE (1997) Dihydrodipicolinate synthase from *Escherichia coli*: pH dependent changes in the kinetic mechanism and kinetic mechanism of allosteric inhibition by L-lysine. Biochemistry 36:1730–1739

Kumpaisal R, Hashimoto T, Yamada Y (1987) Purification and characterization of dihydrodipicolinate synthase from wheat suspension cultures. Plant Physiol 85:145–151

Laber B, Gomis-Ruth FX, Romao MJ, Huber R (1992) *Escherichia coli* dihydrodipicolinate synthase. Identification of the active site and crystallization. Biochem J 288(Pt 2):691–695

Massant J, Verstreken P, Durbecq V, Kholti A, Legrain C, Beeckmans S, Cornelis P, Glansdorff N (2002) Metabolic channeling of carbamoyl phosphate, a thermolabile intermediate: evidence for physical interaction between carbamate kinase-like carbamoyl-phosphate synthetase and ornithine carbamoyltransferase from the hyperthermophile Pyrococcus furiosus. J Biol Chem 277:18517–18522

Mazelis M, Whatley FR, Whatley J (1977) The enzymology of lysine biosynthesis in higher plants. The occurrence, characterization and some regulatory properties of dihydrodipicolinate synthase. FEBS Lett 84:236–240

Mirwaldt C, Korndorfer I, Huber R (1995) The crystal structure of dihydrodipicolinate synthase from *Escherichia coli* at 2.5 A resolution. J Mol Biol 246:227–239

Pearce FG, Perugini MA, McKerchar HJ, Gerrard JA (2006) Dihydrodipicolinate synthase from *Thermotoga maritima*. Biochem J 400:359–366

Roberts SJ, Morris JC, Dobson RC, Gerrard JA (2003) The preparation of (*S*)-aspartate semi-aldehyde appropriate for use in biochemical studies. Bioorg Med Chem Lett 13:265–267

Scapin G, Reddy SG, Zheng R, Blanchard JS (1997) Three-dimensional structure of *Escherichia coli* dihydrodipicolinate reductase in complex with NADH and the inhibitor 2,6-pyridinedicarboxylate. Biochemistry 36:15081–15088

Shedlarski JG, Gilvarg C (1970) The pyruvate-aspartic semialdehyde condensing enzyme of *Escherichia coli*. J Biol Chem 245:1362–1373

Stahly DP (1969) Dihydrodipicolinic acid synthase of *Bacillus licheniformis*. Biochim Biophys Acta 191:439–451

Tam PH, Phenix CP, Palmer DR (2004) MosA, a protein implicated in rhizopine biosynthesis in *Sinorhizobium meliloti* L5-30, is a dihydrodipicolinate synthase. J Mol Biol 335:393–397

Tsujimoto N, Gunji Y, Ogawa-Miyata Y, Shimaoka M, Yasueda H (2006) L-Lysine biosynthetic pathway of *Methylophilus methylotrophus* and construction of an L-Lysine producer. J Biotechnol 124:327–337

Tudor DW, Lewis T, Robins DJ (1993) Synthesis of the Trifluoroacetate salt of aspartic-acid beta-semialdehyde, an intermediate in the biosynthesis of L-Lysine, L-Threonine, and L-Methionine. Synthesis-Stuttgart: 1061–1062

Vauterin M, Jacobs M (1994) Isolation of a poplar and an *Arabidopsis thaliana* dihydrodipicolinate synthase cDNA clone. Plant Mol Biol 25:545–550

Vieille C, Hess JM, Kelly RM, Zeikus JG (1995) xylA cloning and sequencing and biochemical characterization of xylose isomerase from *Thermotoga neapolitana*. Appl Environ Microbiol 61:1867–1875

Wang F, Blanchard JS, Tang XJ (1997) Hydrogen exchange/electrospray ionization mass spectrometry studies of substrate and inhibitor binding and conformational changes of *Escherichia coli* dihydrodipicolinate reductase. Biochemistry 36:3755–3759

Wernic D, Dimaio J, Adams J (1989) Enantiospecific synthesis of L-alpha-aminosuberic acid—synthetic applications in preparation of atrial natriuretic factor analogs. J Org Chem 54:4224–4228

Wolterink-van Loo S, van Eerde A, Siemerink MA, Akerboom J, Dijkstra BW, van der Oost J (2007) Biochemical and structural exploration of the catalytic capacity of sulfolobus KDG aldolases. Biochem J 403:421–430

Xue Y, Xu Y, Liu Y, Ma Y, Zhou P (2001) *Thermoanaerobacter tengcongensis* sp. nov., a novel anaerobic, saccharolytic, thermophilic bacterium isolated from a hot spring in Tengcong, China. Int J Syst Evol Microbiol 51:1335–1341

Yugari Y, Gilvarg C (1965) The condensation step in diaminopimelate synthesis. J Biol Chem 240:4710–4716

Ziegenhorn J, Senn M, Bucher T (1976) Molar absorptivities of beta-NADH and beta-NADPH. Clin Chem 22:151–160